American Journal of Networks and Communications
2024; 13(2): 97-107
http://www.sciencepublishinggroup.com/j/ajnc
doi: 10.11648/j.ajnc.20241302.12
ISSN: 2326-893X (Print); ISSN: 2326-8964 (Online)

Detection of Practical Primary Users in Severe Noise Environments for Cognitive Radio

Mousumi Haque[1, *], Yosuke Sugiura[2], Tetsuya Shimamura[2]

[1]Information and Communication Engineering, University of Rajshahi, Rajshahi, Bangladesh
[2]Graduate School of Science and Engineering, Saitama University, Saitama, Japan

Email address:

mouice@ru.ac.bd (Mousumi Haque), ysugiura@mail.saitama-u.ac.jp (Yosuke Sugiura), shima@mail.saitama-u.ac.jp (Tetsuya Shimamura)
[*]Corresponding author

To cite this article:

Mousumi Haque, Yosuke Sugiura, Tetsuya Shimamura. (2024). Detection of Practical Primary Users in Severe Noise Environments for Cognitive Radio. *American Journal of Networks and Communications, 13*(2), 97-107. https://doi.org/10.11648/j.ajnc.20241302.12

Received: 21 August 2024; **Accepted:** 18 September 2024; **Published:** 31 October 2024

Abstract: Cognitive radio (CR) is one of the compelling ideas to solve the spectrum scarcity problem for rapid developments in wireless communication systems. In CR systems, signal detection for orthogonal frequency division multiplexing (OFDM) systems in severe noise environments is a key challenge. The area of practical primary user detection has not been explored in depth. The proposed method is an effective method for sensing OFDM applications, which are the practical primary users, for low signal-to-noise (SNR) cases. In the proposed method, the parallel combination of the comb filter and the time-domain autocorrelation function is exploited. The detection performance is measured for various OFDM system applications, including the IEEE 802.11a wireless LAN (WLAN) radio interface, long-term evaluation (LTE), and digital audio broadcasting (DAB) for various CP ratios under 16-quadrature amplitude modulation (16-QAM) and 64-quadrature amplitude modulation (64-QAM) over multipath Rayleigh fading channels with additive white Gaussian noise (AWGN). Furthermore, the OFDM sensing is possible in the presence of noise uncertainty and the sensing performance is compared under consideration with and without noise uncertainty cases. The simulation results demonstrated that our proposed method undoubtedly improves the sensing performances (up to 11 dB SNR gain) of practical primary users more than the conventional spectrum detection methods for low SNR cases.

Keywords: WLAN, LTE, DAB, Noise Uncertainty, SNR, Cognitive Radio

1. Introduction

Cognitive radio (CR) is an effective and reliable solution for the efficient use of the radio frequency spectrum [1]. CR is based on the premise that OnTheMove, environment-aware computing, and related research will create innovative applications that can use location and other aspects of the environment to tailor services to users. Therefore, CR incorporates machine learning methods that improve robustness to rapidly changing external environments [2]. The spectrum scarcity is a significant constraint because of the rapid development of numerous multimedia applications using advanced wireless communication systems over the previous decade. In CR systems, signal detection plays an important role in preventing spectrum scarcity by investigating spectrum vacancies for future and modern wireless communication systems. There are two types of spectrum sensing techniques: cooperative spectrum sensing [3–7] and non-cooperative spectrum sensing [8–10]. Numerous spectrum sensing methods have been proposed during the last few years [11–19]. Cyclostationary features were used for sensing the signal [20]. Matched filter detection enables the most effective sensing performance, when previous knowledge about the primary user signal is available [21, 22]. An energy detector is one of the most commonly used semi-blind spectrum sensing methods, which does not require prior knowledge of the primary user signal [23–25]. However, the performance of the energy detector is not good in severe noise environments. The blind spectrum sensing technique operates without prior knowledge of the signal or noise power [26], yet it proves ineffective in scenarios where the signal-to-noise ratio (SNR)

is low.

Correlation-based spectrum sensing methods are highly favored because they exhibit low computational complexity and perform well over fading channels [27, 28]. Utilizing the autocorrelation property in the time domain of cyclic prefix (CP) based orthogonal frequency division multiplexing (OFDM) signals enabled spectrum sensing [29, 30]. This approach employed a particularly small fast Fourier transform (FFT) for OFDM-transmitted signals. Furthermore, the detection performance is not very good for low SNR cases. In addition, this method was extended and used large FFT sizes in [31]. In contrast, it is understood that the issue of carrier frequency offset due to large FFT sizes disrupts orthogonality in OFDM, thereby diminishing the spectrum sensing detection performance [31]. Recently, Chin et al. [32] proposed a spectrum sensing method for OFDM signals over multipath fading channels considering noise uncertainty environments. A very small size of FFT is considered in this method. However, the detection performance is not very good for low SNR cases. A signal detection approach was proposed for the improvement of SNR in [33]. The detection performance is good under quadrature phase shift keying (QPSK), but this method did not consider 16-QAM and 64-QAM for the DVB-T2 signal, which are very important parameters for DVB-T2 systems. Furthermore, in this method, the effect of noise uncertainty, which is an unavoidable parameter for signal detection in severe noise environments, was not investigated. The suggested approach resolves the primary drawback of the outcomes of the current spectrum sensing approaches.

This study improves the OFDM-based applications' detection performance in low SNR scenarios. The current wireless communication systems make extensive use of OFDM. The CP is used to mitigate inter symbol interference (ISI). For OFDM-based systems, various CP sizes (1/32, 1/16, 1/8, and 1/4), FFT sizes, and digital modulation schemes are used. As a result, sensing performance improvement in severe noise environments for OFDM-based applications is a very important task in CR systems. In the proposed method, the detection performance is evaluated of various OFDM system applications, including wireless LAN (WLAN) radio interface IEEE 802.11a, long-term evaluation (LTE), and digital audio broadcasting (DAB) for different CP sizes under higher-order digital modulation schemes, 16-quadrature amplitude modulation (16-QAM) and 64-quadrature amplitude modulation (64-QAM), over multipath fading channels with additive white Gaussian noise (AWGN). Furthermore, the OFDM systems sensing is possible in the presence of noise uncertainty and the OFDM sensing performance is compared under consideration with and without noise uncertainty cases. The combination of comb filter and time domain autocorrelation calculation is applied in a parallel form for sensing OFDM transmitted signals. No prior information about the primary users is essential in this method, but noise variance is used for sensing. Therefore, this method is semi-blind spectrum sensing. The detection performance of spectrum sensing is increased by improving effectively the SNR of the received signal. The proposed method is compared with the conventional state-of-the-art method over multipath Rayleigh fading channels [30, 32]. Simulation results demonstrated that our proposed spectrum sensing method markedly improved the sensing performance.

The rest of the paper is organized as follows. Section II describes the system model of spectrum sensing for OFDM-transmitted signals. Section III provides a short description of the use of OFDM-transmitted signals for spectrum sensing. A detailed mathematical explanation of the proposed method is presented in Section IV. Section V gives spectrum sensing performance evaluation and compares it with the state-of-the-art method. Finally, in Section VI, a conclusion of this paper is drawn.

2. System Methodology

In the spectrum sensing model, the two hypotheses are defined by the idle state, H_0, and active state, H_1. The secondary user's receiver evaluates a test statistic, T_f, based on its observed signal and compares it with a specific threshold, λ, to decide the situation between the two hypotheses. The two hypotheses are given by

$$H_0 : T_f < \lambda \tag{1}$$

$$H_1 : T_f \geq \lambda\,. \tag{2}$$

The probability of detection, P_d, indicates the primary user correctly detects its active mode [21] as

$$P_d = P(H_1; H_1) = Pr\{\, T_f > \lambda \,\|\, H_1 \,\}\,. \tag{3}$$

There are two types of errors: the probability of false alarm, P_{fa}, and the probability of miss detection, P_m. These can be given [21] as

$$P_{fa} = P(H_1; H_0) \tag{4}$$

$$P_m = P(H_0; H_1)\,. \tag{5}$$

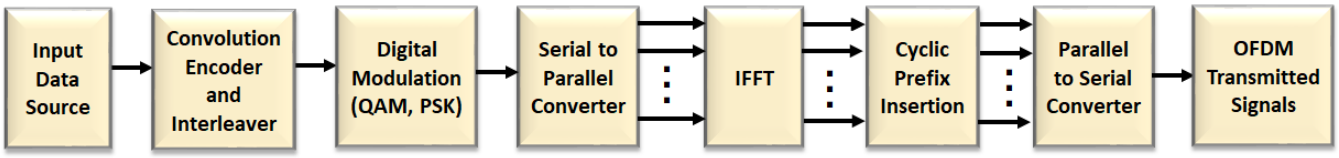

Figure 1. *Block diagram of OFDM systems.*

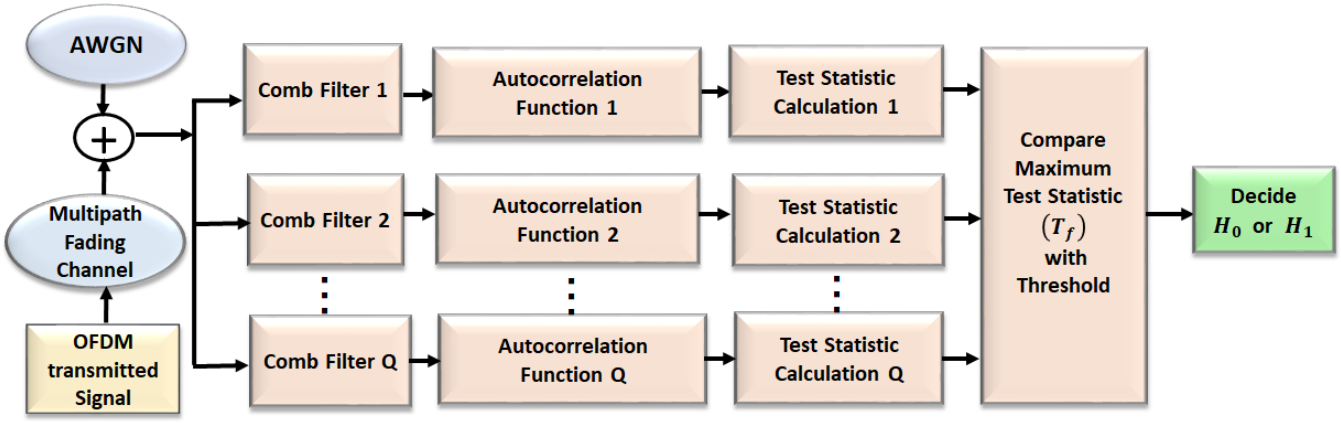

Figure 2. *Block diagram of proposed spectrum sensing method.*

3. OFDM Systems as Primary User

This method considers OFDM-transmitted signals as the primary user. An OFDM signal received at the sensing station serves as the primary user signal. The large FFT size OFDM signal is assumed to be received by being passed through a multipath Rayleigh fading channel. OFDM is a multicarrier modulation in which the input data streams are convolutionally encoded by a convolutional encoder of rated $1/2$ and the interleaver is used to combat errors that occur in bursts. Figure 1 shows a block diagram of the OFDM systems. The encoded bits are digitally modulated, resulting in a complex symbol stream $X(0), X(1), ..., X(N-1)$. This symbol stream is converted to parallel subchannels, which are the frequency components, and converted into time samples taking the inverse fast Fourier transform (IFFT). The IFFT gives the OFDM symbol consisting of the sequence $x(0), x(1), ..., x(N-1)$ of length N as

$$IFFT\{X(k)\} = x(n) = \frac{1}{\sqrt{N}} \sum_{k=0}^{N-1} X(k) e^{j2\pi kn/N} \quad (6)$$

The CP for $x(n)$ can be defined by $x(N-C), ..., x(N-1)$ where it consists of the last C samples of the $x(n)$ sequence. For each input sequence of length N, these last C samples are appended at the beginning of the sequence. This gives a new sequence, $\tilde{x}(n)$, of length $M = N + C$ of each OFDM symbol that is converted by a parallel-to-serial converter.

The transmitted signal is filtered by the channel impulse response $h(n)$ and corrupted by the additive noise $w(n)$. Consider the P order multipath channel and the channel tap coefficients $h(u)$, for $u = 0, 1, ..., P-1$. Finally, the received signal is given by

$$\begin{aligned} y(n) &= \tilde{x}(n) * h(n) + w(n) \\ &= \textstyle\sum_{u=0}^{P-1} h(u)\tilde{x}(n-u) + w(n) \\ &= s(n) + w(n) \end{aligned} \quad (7)$$

where the asterisk denotes convolution and $s(n) = \sum_{u=0}^{P-1} h(u)\tilde{x}(n-u)$ is used for simplicity.

4. Proposed Method

In the proposed method, OFDM-based applications are used as primary user transmitters. In this paper, parallel comb filters are employed to reduce the loss of orthogonality of an OFDM signal, and the autocorrelation functions in each parallel channel are averaged and enhanced for spectrum sensing. Figure 2 shows a block diagram of the proposed spectrum sensing method. In the proposed method, the transmitted OFDM signal is considered as the primary user and the received spectrum sensing is used as the secondary user.

For H_0, OFDM transmitted signal is absent and the OFDM transmitted signal is present for H_1 which can be described by

$$H_0 : y(n) = w(n) \quad (8)$$

$$H_1 : y(n) = s(n) + w(n). \quad (9)$$

In the proposed method, finite impulse response (FIR) comb filters are used whose frequency response constructs a series of regularly spaced notches. The synchronization problems of the OFDM symbol can be reduced by the comb filter [35]. The filter output of the p_{th} comb filter from the l_{th} OFDM symbol input, $f_{p,l}(n)$, is described [35], [36] by

$$f_{p,l}(n) = y_{p,l}(n) + g_p\, y_{p,l}(n-K) \quad (10)$$

where $1 \le l \le S$, K the delay length of the p_{th} filter and g_p is the filter coefficient of the p_{th} filter, given by

$$g_p = e^{\,j2\pi\, p\, \lfloor N/Q \rfloor /N} \quad (11)$$

where $\lfloor \cdot \rfloor$ is a floor function and Q corresponds to the number of comb filters used in a parallel form.

In (10), $y_{p,l}(n)$ represents the l_{th} OFDM symbol input for the p_{th} comb filter can be described for H_1

$$H_1 : y_{p,l}(n) = s_{p,l}(n) + w_{p,l}(n). \quad (12)$$

where $s_{p,l}(n) = \sum_{u=0}^{P-1} h_{p,l}(u)\tilde{x}_{p,l}(n-u)$ and $w_{p,l}(n)$ is the additive noise of the p_{th} comb filter.

Combining (10) and (12), $f_{p,l}(n)$ for H_1 can be rewritten as

$$H_1 : f_{p,l}(n) = s_{p,l}(n) + w_{p,l}(n) + s_{p,l}(n-K) + w_{p,l}(n-K) \quad (13)$$

where g_p is set as 1 when $p = 0$ is considered in (11). This case is considered for a single filter. Here, this value is used for the simplicity of the calculation.

The output signal of the p_{th} comb filter for each OFDM symbol is used as the input to the time domain symbol autocorrelation function. The autocorrelation function calculation of the l_{th} OFDM symbol for the p_{th} comb filter output, $R_{p,l}(\tau)$, is described by

$$R_{p,l}(\tau) = \frac{1}{M}\sum_{n=0}^{M-1} f_{p,l}(n) f^*_{p,l}(n+\tau) \quad (14)$$

where $1 \le p \le Q$, τ is the lag number from 0 to $(M-1)$, M is the number of samples and $(.)^*$ denotes the complex conjugate of the values. Combining (13) and (14), the $R_{p,l}(\tau)$ can be written for H_1 as

$$\begin{aligned} H_1 : R_{p,l}(\tau) = \tfrac{1}{M}\textstyle\sum_{n=0}^{M-1}[\{s_{p,l}(n) + w_{p,l}(n) + s_{p,l}(n-K) \\ +w_{p,l}(n-K)\}\{s^*_{p,l}(n+\tau) + w^*_{p,l}(n+\tau) + s^*_{p,l}(n-K+\tau) + w^*_{p,l}(n-K+\tau)\}] \end{aligned} \quad (15)$$

Independence of channel taps $h(u)$ and $\tilde{x}(n)$ gives

$$\begin{aligned} R_{ss}(\tau) &= \tfrac{1}{M}\textstyle\sum_{n=0}^{M-1}[s_{p,l}(n)s^*_{p,l}(n+\tau)] \\ &= \tfrac{1}{M}\textstyle\sum_{n=0}^{M-1}[\sum_{u=0}^{P-1}(h_{p,l}(u)\tilde{x}_{p,l}(n-u))\sum_{u=0}^{P-1}(h^*_{p,l}(u)\tilde{x}^*_{p,l}(n-u+\tau))] \\ &= \tfrac{1}{M}\textstyle\sum_{n=0}^{M-1}\sum_{u=0}^{P-1}[h_{p,l}(u)h^*_{p,l}(u)]\tfrac{1}{M}\sum_{n=0}^{M-1}\sum_{u=0}^{P-1}[\tilde{x}_{p,l}(n-u)\tilde{x}^*_{p,l}(n-u+\tau)] \\ &= \delta\sigma_x^2. \end{aligned} \quad (16)$$

where $\delta = \frac{1}{M}\sum_{n=0}^{M-1}\sum_{u=0}^{P-1}[h_{p,l}(u)h^*_{p,l}(u)]$ is used for simplicity and σ_x^2 is the signal variance.

Similarly, $s_{p,l}(n)$ is not correlated with $w_{p,l}(n)$. Furthermore, $w_{p,l}(n)$ are not correlated with each other, except for $\tau = 0$. From (15) and (16), the $R_{p,l}(\tau)$ can be written as

$$H_1 : R_{p,l}(\tau) = 2\delta\sigma_x^2 \; ; \; when \; (\tau \neq 0) \quad (17)$$

$$\begin{aligned} H_1 : R_{p,l}(\tau) &= 2(R_{ss}(\tau) + R_{ww}(\tau)) \\ &= 2(\delta\sigma_x^2 + \sigma_w^2) \; ; \; when \; (\tau = 0) \end{aligned} \quad (18)$$

where $R_{ss}(\tau)$ and $R_{ww}(\tau)$ are the autocorrelation function of $s(n)$ and $w(n)$, and σ_w^2 is the variance of $w(n)$.

In the conventional method, the autocorrelation coefficient is expressed [30] by

$$\rho(\tau) = \frac{\frac{1}{M}\sum_{n=0}^{M-1}[y(n)y^*(n+N)\,1\,H_1]}{\frac{1}{M}\sum_{n=0}^{M-1}[y(n)y^*(n)\,1\,H_1]} \quad (19)$$

From (19), the conventional method autocorrelation coefficient, $\rho_c(\tau)$, is expressed [30] by

$$\rho_c(\tau) = \frac{C}{N+C}\frac{\delta\sigma_x^2}{\delta\sigma_x^2+\sigma_w^2} \quad (20)$$

Similarly, from (19), the proposed method autocorrelation coefficient, $\rho_r(\tau)$, can be written as

$$\rho_r(\tau) = \frac{\frac{1}{M}\sum_{n=0}^{M-1}[f_{p,l}(n)f^*_{p,l}(n+\tau)\,1\,H_1]}{\frac{1}{M}\sum_{n=0}^{M-1}[f_{p,l}(n)f^*_{p,l}(n)\,1\,H_1]} \quad (21)$$

Substituting (17) and (18) in (21), the $\rho_r(\tau)$ is rewritten as

$$\begin{aligned} \rho_r(\tau) &= \frac{R_{p,l}(\tau)\;;\;when\;(\tau\neq 0)}{R_{p,l}(\tau)\;;\;when\;(\tau=0)} \\ &= \frac{\delta\sigma_x^2}{\delta\sigma_x^2+\sigma_w^2} \end{aligned} \quad (22)$$

From (20) and (22), the $\rho_r(\tau)$ can be written as

$$\rho_r(\tau) = (\frac{N+C}{C})\rho_c(\tau) \quad (23)$$

It can be seen from (23) that $\rho_r(\tau) > \rho_c(\tau)$. In other words, the autocorrelation coefficient of the proposed method is greater than that of the conventional method. The detection performance of the proposed method increases more than that of the conventional method. The autocorrelation function

is used to detect OFDM-transmitted signals in severe noise environments.

In our proposed scheme, the autocorrelation calculation of all OFDM symbols with $1 \leq l \leq S$ is used to select the test statistic for the detection of the primary user. Each test statistic, T_p, is measured by averaging each autocorrelation function in each path can be obtained by

$$T_p = \sum_{l=1}^{S} \bar{R}_{p,l}(\tau) \tag{24}$$

where $\bar{R}_{p,l}(\tau)$ is the average value of autocorrelation function of (14), given by

$$\bar{R}_{p,l}(\tau) = \frac{1}{M} \sum_{\tau=0}^{M-1} \|R_{p,l}(\tau)\| \tag{25}$$

The maximum value among all the T_ps is used as the final test statistic T_f can be expressed by

$$T_f = [T_p]_{max} \tag{26}$$

where $[\cdot]_{max}$ is a maximum function.

The threshold value is obtained from the noise variance σ_w^2 as a priori information from the channel, where the technique in [34] is available for example. Calculate the threshold value λ [36] as

$$\lambda = \sqrt{-\ln P_{fa} \cdot \sigma_w^2}. \tag{27}$$

The noise uncertainty, ζ, is measured in dB [37] as

$$\zeta = 10 \log_{10} \Psi. \tag{28}$$

where $\Psi > 1$ is a parameter that estimates the noise uncertainty [37].

In our proposed spectrum sensing method, when the influence of noise uncertainty is considered, the threshold value λ is calculated from Eq. (27) using $\Psi\sigma_w^2$ instead of σ_w^2.

Finally, the cognitive controller or receiver gives the final output H_0 or H_1 from (1) and (2).

It is very important to ensure the sensing of the OFDM signal in severe noise environments, which is accomplished by the proposed semi-blind spectrum sensing method.

5. Simulation Results and Discussions

The performance is examined for many OFDM applications, such as the WLAN radio interface IEEE 802.11a, LTE, and DAB, in order to appraise the suggested technique. Through MATLAB simulations, this approach is compared with the traditional approaches. Table 1 contains the simulation parameters that were utilized in the study, with the definition of the CP ratio being $N_c = C/N$, unless otherwise indicated. The five tap impulse response in the multipath Rayleigh fading channel has a maximum delay of eight.

Table 1. *Simulation parameters.*

Parameters	Types
OFDM Application	WLAN, LTE, DAB
Digital Modulation	16-QAM, 64-QAM
FFT Size N	Depend upon OFDM Application
Number of OFDM Symbols S	140
Probability of False Alarm P_{fa}	0.01, 0.05, 0.1, 0.2
CP Ratio N_c	Depend upon OFDM Application
Channel	Multipath Rayleigh Fading with AWGN
SNR Range	-35 dB to 0 dB
Number of Comb Filters Q	3
Number of Iterations	1500

5.1. Performance Evaluation

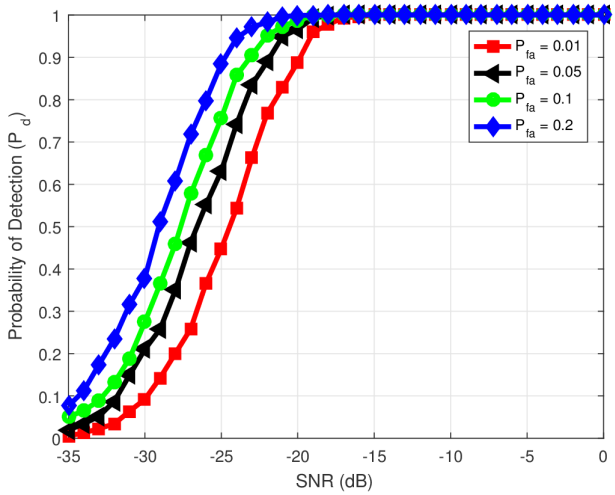

Figure 3. *Spectrum Sensing of WLAN under 16-QAM.*

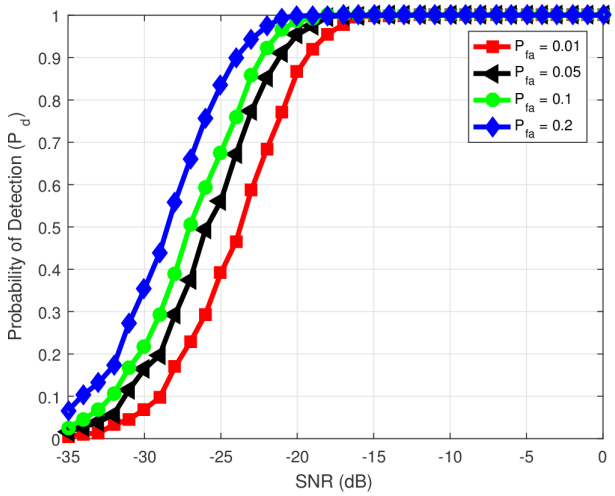

Figure 4. *Spectrum Sensing of LTE under 16-QAM.*

The probability of detection P_d of the WLAN system for various probability of false alarm P_{fa} is shown in Figure 3. Here, the size of FFT 64 and N_c 1/4 are considered for sensing the primary user. When the P_{fa} increases, sensing performance increases with SNR. It is shown that for very low P_{fa} which is 1%, the maximum P_d is achieved at -19 dB. Moreover, when P_{fa} is 20%, the maximum P_d is achieved at -24 dB SNR. The maximum P_d in severe noise environments is obtained for the WLAN system using the proposed method.

Figure 4. presents the P_d of the LTE system under 16-QAM for different P_{fa}. The size of FFT is 512 and the CP is chosen as 36 for the LTE system. The maximum P_d is achieved at -19 dB for 1% P_{fa}, -21 dB for 5% P_{fa}, -22 dB for 10% P_{fa} and -24 dB for 20% P_{fa}. The P_d increases with SNR and P_{fa}. These findings demonstrate that the suggested spectrum sensing strategy leads to a considerable improvement in sensing performance as P_{fa} increases.

For the performance evaluation of the proposed spectrum sensing, the P_d of the DAB system for N_c 1/32 is presented in Figure 5. The fixed P_{fa} determines how gradually the P_d grows with SNR. The maximum P_d ($\geq$ 0.9 or 90%) is reached in a very low SNR environment (-16 dB) with extremely low P_{fa}, which is 1%. The maximum P_d is obtained at -18 dB SNR for 5% P_{fa}. In addition, when P_{fa} is 10%, P_d increases. Here, the maximum P_d is achieved in a low SNR environment (-19 dB), indicating a 3 dB SNR improvement over 1% P_{fa}. Finally, the primary user detection performance increases dramatically for 20% P_{fa}. It is highly observable that the sensing performance with the suggested technique improves dramatically with increasing P_{fa}.

The P_d of DAB system for N_c 1/16 is shown in Figure 6. Here, sensing performance utilizing the suggested technique grows with SNR as the P_{fa} increases. The detection performance for the 20% P_{fa} outperforms the 1%, 5%, and 10% P_{fa}. It is clear that for very low P_{fa} which is 1%, the maximum P_d ($\geq$ 0.9 or 90%) is achieved in a very low SNR environment (-16 dB). Figure 7 presents the P_d of DAB system for N_c 1/8 for various P_{fa}. Spectrum sensing can be accomplished in any scenario at a variety of SNRs. In situations with low SNR, the P_d of CP-OFDM signals is excellent for extremely low P_{fa} 1%.

The P_d of the DAB transmitted signals is presented for N_c 1/4 in Figure 8. The P_d increases with SNR as well as P_{fa}. The maximum P_d is achieved at -15 dB for 1% P_{fa}, -17 dB for 5% P_{fa}, -18 dB for 10% P_{fa}, and -20 dB for 20% P_{fa}. For 16-QAM modulation, the P_d increases with SNR as well as P_{fa}. In extreme noise situations, P_d performs admirably across a range of CP sizes, which is crucial for OFDM-based systems. The P_d of 1/4 CP-based DAB transmitted signals for various P_{fa} under 64-QAM is represented in Figure 9. For different P_{fa}, the P_d increases at a wide range of SNR. Many OFDM-based systems are using 64-QAM. The maximum P_d for low SNR cases is very much important that is obtained using the proposed method.

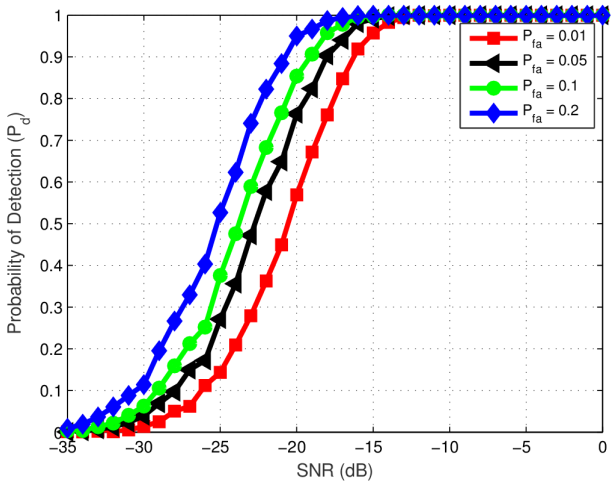

Figure 5. *Spectrum Sensing of DAB under 16-QAM for N_c 1/32.*

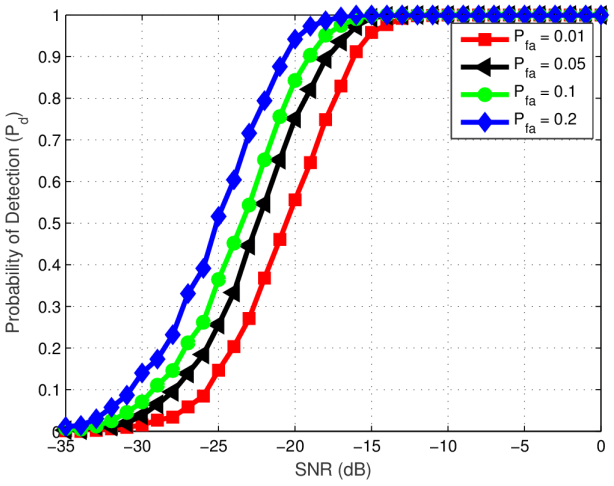

Figure 6. *Spectrum Sensing of DAB under 16-QAM for N_c 1/16.*

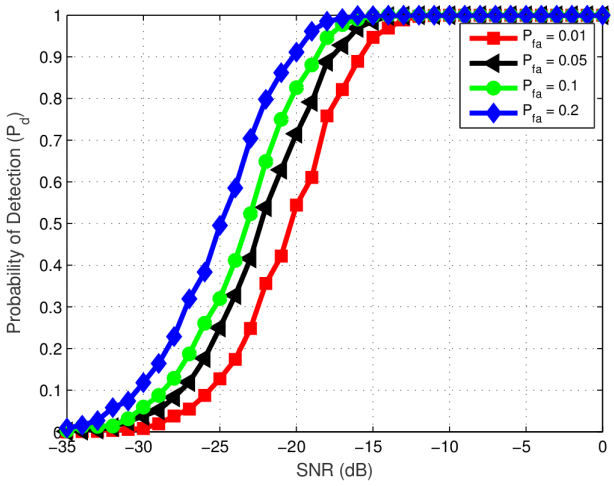

Figure 7. *Spectrum Sensing of DAB under 16-QAM for N_c 1/8.*

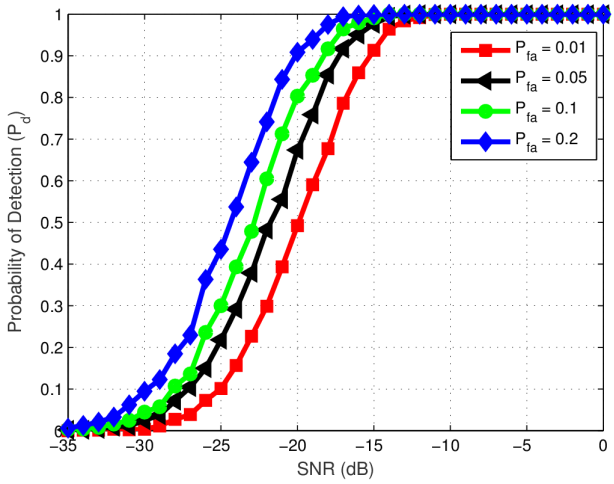

Figure 8. *Spectrum Sensing of DAB under 16-QAM for N_c 1/4.*

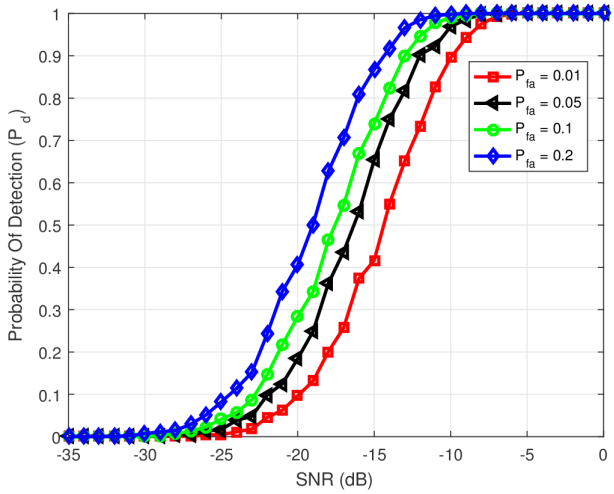

Figure 9. *Spectrum Sensing of DAB under 64-QAM.*

Noise uncertainty is a very important parameter for the evaluation of spectrum sensing performance. In the proposed signal detection, the effect of noise uncertainty to detect the primary user signal is analyzed at fixed P_{fa} 0.01 under 16-QAM for performance evaluation. Figure 10 shows the detection performance of DAB signals for N_c 1/4 under 0.5 dB, 1 dB, and 1.5 dB noise uncertainty. It is clear from Figure 10 that when the noise uncertainty increases, the probability of detecting primary user signal P_d decreases slightly with SNR. However, the proposed signal detection method shows that maximum P_d ($\geq 90\%$) is achieved at SNR -20 dB and -19 dB with noise uncertainties of 0.5 dB and 1.5 dB, which is very important for signal detection in CR for wireless communication systems.

In the proposed method, the CP ratios 1/8 and fixed P_{fa} 0.01 and 16-QAM are considered to analyze the effect of noise uncertainty. The P_d of DAB signals in cases of 0.5 dB, 1 dB, and 1.5 dB noise uncertainties are shown in Figure 11. The plot shows that as the noise uncertainty rises, there is a slight decrease in the probability of detecting the primary user signal with respect to the SNR. On the other hand, the P_d of our proposed method shows the satisfactory result with 0.5 dB, 1 dB, and 1.5 dB noise uncertainties for this method.

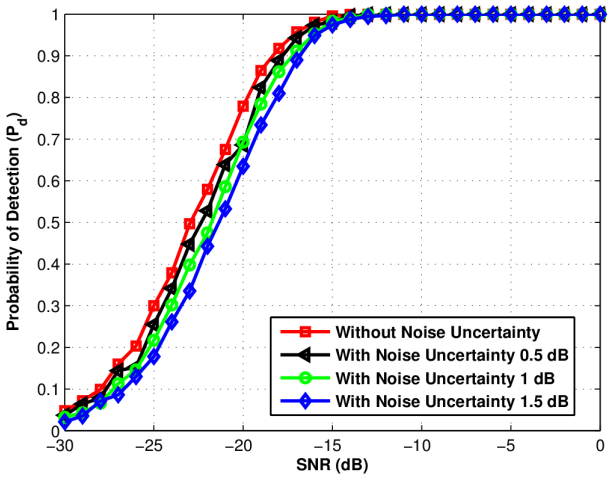

Figure 10. *Spectrum Sensing of DAB for N_c 1/4 with and without noise uncertainty.*

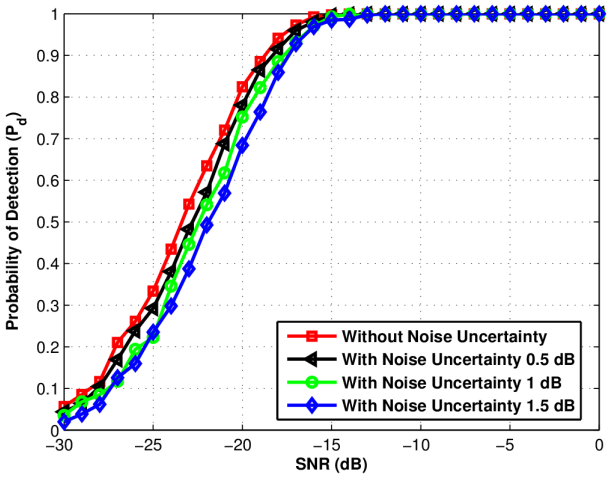

Figure 11. *Spectrum sensing of DAB for N_c 1/8 with and without noise uncertainty.*

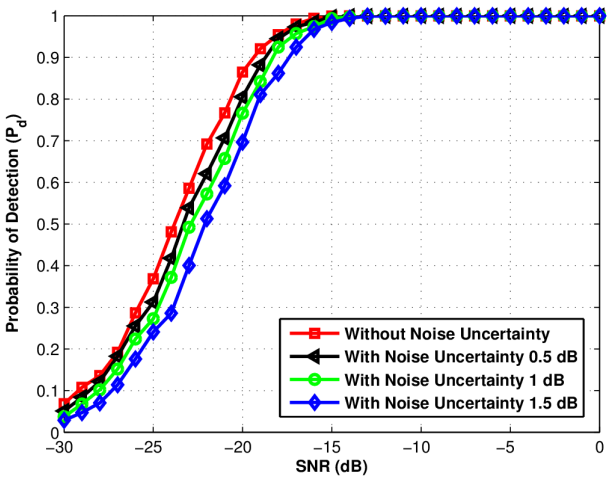

Figure 12. *Spectrum sensing of DAB for N_c 1/16 with and without noise uncertainty.*

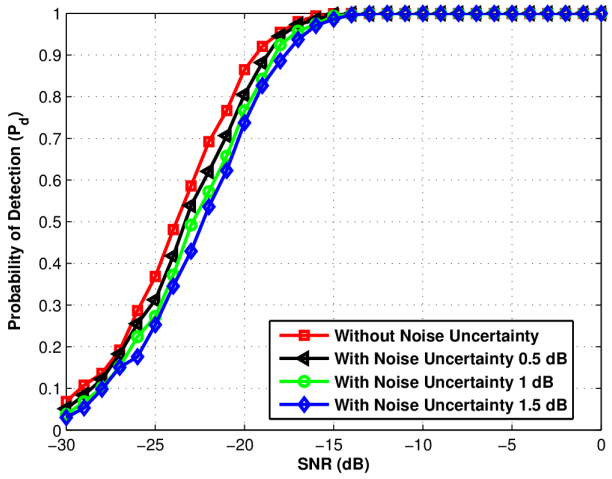

Figure 13. *Spectrum sensing of DAB for N_c 1/32 with and without noise uncertainty.*

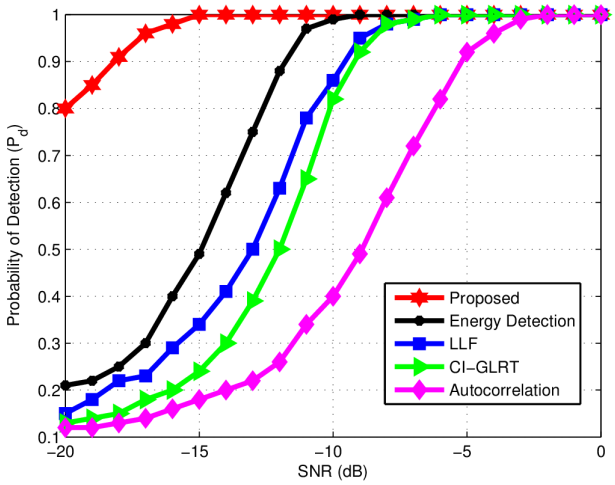

Figure 15. *Performance comparison at fixed P_{fa} of 0.1.*

In Figures 12 and 13, the noise uncertainty 0.5 dB, 1 dB, and 1.5 dB are considered to detect the DAB for CP ratio 1/16, and 1/32, respectively. All the graphs demonstrate that the P_d of the proposed method decreases slightly with increasing noise uncertainty relative to the SNR. However, the satisfactory P_d of the primary user signal is sustained even for 1.5 dB noise uncertainty in highly noisy environments.

5.2. Performance Comparison

The proposed spectrum sensing scheme is compared with the CP autocorrelation-based spectrum sensing method [30]. For the conventional method, the simulation parameters were the size of FFT 32, the CP ratio 1/4, 16-QAM modulation, and P_{fa} 0.05.

Figure 14 represents the effect of receiver operating characteristics (ROC) curves for the proposed method and the conventional method at different levels of signal strength. It is demonstrated from this figure that for the proposed method, P_d increases dramatically at SNR -10 dB, SNR -16 dB, and SNR -21 dB relative to the conventional spectrum sensing scheme.

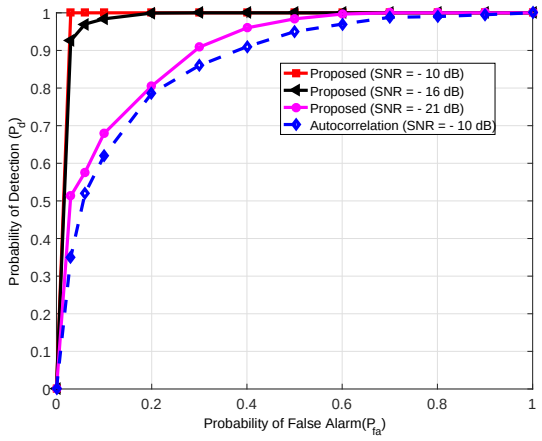

Figure 14. *Performance comparison using ROC curves under 16-QAM.*

The proposed method is compared with the conventional spectrum sensing method [32] in Figure 15. The simulation parameters of this sensing method are an FFT size (N) of 64, the CP ratio (N_c) 1/4, and P_{fa} 0.1. Here, CP-based detectors are considered, namely the energy detector, log-likelihood function (LLF), channel-independent generalized log-likelihood ratio test (CI-GLRT) and autocorrelation detectors. In our proposed method, we consider the CP ratio (N_c) 1/4, and P_{fa} 0.1 for performance comparison. The P_d of the suggested technique is significantly larger than that of the traditional system, as seen in Figure 15.

Table 2 illustrates the detection performance of OFDM-transmitted signals using both traditional and suggested spectrum sensing approaches. The results presented in Table 2 demonstrate that the suggested spectrum-sensing scheme outperforms the energy detection method by 5 dB, the LLF by 8 dB, the CI-GLRT by 9 dB, and the autocorrelation based spectrum-sensing scheme by 13 dB. It is clear from Table 2 that the proposed spectrum-sensing scheme provides a 5 dB SNR improvement compared with that of the energy detection, an 8 dB SNR gain compared with that of the LLF, a 9 dB SNR gain compared with that of the CI-GLRT, and a 13 dB SNR gain compared with that of the autocorrelation based spectrum-sensing scheme respectively.

Table 2. *Probability of detection (P_d) at fixed SNR for proposed and conventional methods.*

Spectrum-Sensing Method	P_d	SNR (dB)
Proposed	1	-15
Energy Detection	1	-10
LLF	1	-7
CI-GLRT	1	-6
Autocorrelation	1	-2

Figure 16 represents the performance comparison of the proposed method and conventional method [32] in the presence of noise uncertainty. The simulation parameters of this sensing method are an FFT size (N) of 64, the CP ratio

(N_c) 1/4, P_{fa} 0.1, and noise uncertainty 0.5 dB. Here, the energy detector, LLF, CI-GLRT, and autocorrelation detectors are considered. In our proposed method, we consider the CP ratio (N_c) 1/4, P_{fa} 0.1, and noise uncertainty 0.5 dB for performance comparison. The P_d of the proposed method dramatically increases than that of the conventional scheme.

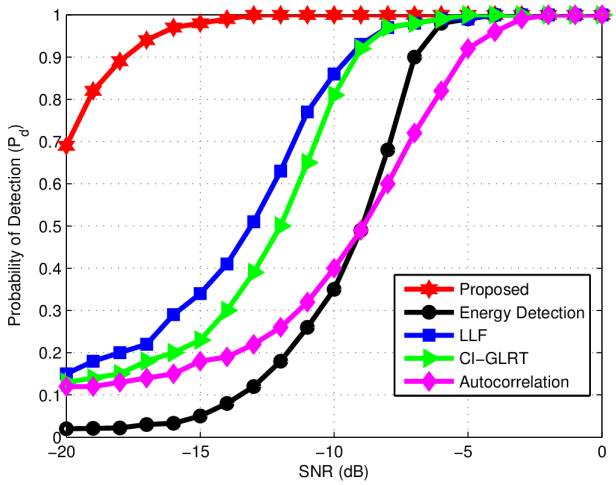

Figure 16. *Performance comparison at fixed P_{fa} of 0.1 and noise uncertainty 0.5 dB.*

Table 3. *Probability of detection (P_d) at fixed SNR for proposed and conventional methods in presence of noise uncertainty 0.5 dB.*

Spectrum-Sensing Method	P_d	SNR (dB)
Proposed	1	-13
Energy Detection	1	-4
LLF	1	-5
CI-GLRT	1	-5
Autocorrelation	1	-2

Table 3 shows the maximum probability of detection for a fixed value of SNR of the proposed and conventional spectrum sensing methods in noise uncertainty for OFDM-transmitted signals. The data presented in Table 3 makes it evident that the suggested spectrum-sensing approach yields superior signal-to-noise ratios (SNR) of 9 dB when compared to energy detection, 8 dB when compared to the LLF, 8 dB when compared to the CI-GLRT, and 11 dB when compared to the autocorrelation based spectrum-sensing method.

6. Conclusion

Taking into consideration the poor sensing performance in severe noise environments, the proposed spectrum sensing is an effective scheme for OFDM-based applications. For sensing OFDM transmitted signals, the parallel combination of comb filter and autocorrelation function is exploited. The proposed method is applicable to various OFDM system applications such as DAB, LTE, and WLAN. This method detects OFDM system applications for various CP ratios under different higher-order digital modulation schemes in the presence of noise uncertainty, which is very important in CR systems. The proposed method improves the spectrum sensing performance dramatically (up to 11 dB SNR gain) of OFDM systems more than the conventional spectrum sensing methods for low SNR cases.

Abbreviations

CR	Cognitive Radio
OFDM	Orthogonal Frequency Division Multiplexing
CP	Cyclic Prefix
WLAN	Wireless LAN
LTE	Long Term Evaluation
DAB	Digital Audio Broadcasting
FFT	Fast Fourier Transform
ISI	Inter Symbol Interference
SNR	Signal-to-Noise Ratio
AWGN	Additive White Gaussian Noise
16-QAM	16-Quadrature Amplitude Modulation
64-QAM	64-Quadrature Amplitude Modulation
ROC	Receiver Operating Characteristics

ORCID

0000-0003-3322-6420 (Mousumi Haque)
0000-0002-8415-4482 (Yosuke Sugiura)
0000-0002-7874-3467 (Tetsuya Shimamura)

Author Contributions

Mousumi Haque: Conceptualization, Data curation, Formal Analysis, Investigation, Methodology, Software, Validation, Visualization, Writing - original draft

Yosuke Sugiura: Conceptualization, Data curation, Formal Analysis, Investigation, Supervision, Validation, Writing - review & editing

Tetsuya Shimamura: Conceptualization, Data curation, Funding acquisition, Investigation, Supervision, Validation, Writing - review & editing

Conflicts of Interest

The authors declare that they have no conflicting interests.

References

[1] Mitola, J. *Cognitive radio: an integrated agent architecture for software defined radio*. Ph.D. Dissertation, Royal Institute of Technology, Sweden, 2000.

[2] Haykin, S. Cognitive radio: brain-empowered wireless communications. *IEEE Journal of Selected Areas in Communications*. 2005, 23(2), 201-220. https://doi.org/10.1109/JSAC.2004.839380

[3] Yu, Q. A Survey of Cooperative Games for Cognitive Radio Networks. *Wireless Personal Communications*. 2013, 73, 949-966. https://doi.org/10.1007/s11277-013-1225-6

[4] Huang, H., Mu, J., Jing, X. Cooperative spectrum sensing based on centralized double threshold in MCN. *China Communications*. 2020, 17(5), 235-242. https://doi.org/10.23919/JCC.2020.05.018

[5] Cichon, K., Kliks, A., Bogucka, H. Energy-efficient cooperative spectrum sensing: a survey. *IEEE Communications Surveys and Tutorials*. 2016, 18(3), 1861-1886. https://doi.org/10.1109/COMST.2016.2553178

[6] Lee, W., Kim, M., Cho, D. H. Deep cooperative sensing: cooperative spectrum sensing based on convolutional neural networks. *IEEE Transactions on Vehicular Technology*. 2019, 68(3), 3005-3009. https://doi.org/10.1109/TVT.2019.2891291

[7] Verma, G., Sahu, O. P. A Distance Based Reliable Cooperative Spectrum Sensing Algorithm in Cognitive Radio. *Wireless Personal Communications*. 2018, 99, 203-212. https://doi.org/10.1007/s11277-017-5052-z

[8] Huang, X. L., Xu, Y., Wu, J., Zhang, W. Non-cooperative spectrum sensing with historical sensing data mining in cognitive radio. *IEEE Transactions on Vehicular Technology*. 2017, 66(10), 8863-8871. https://doi.org/10.1109/TVT.2017.2698206

[9] Pati, B. M., Kaneko, M., Taparugssanagorn, A. A deep convolutional neural network based transfer learning method for non-cooperative spectrum sensing. *IEEE Access*. 2020, 8, 164529-164545. https://doi.org/10.1109/ACCESS.2020.3022513

[10] Bouallegue, K., Crussiere, M., Kharbech, S. SVM assisted primary user-detection for non-cooperative cognitive radio networks. *In IEEE Symposium on Computers and Communications (ISCC)*. Rennes, France, 2020. https://doi.org/10.1109/ISCC50000.2020.9219601

[11] Singh, A. K., Ranjan, R. Multiâlayer perceptron based spectrum prediction in cognitive radio network. *Wireless Personal Communications*. 2022, 123, 3539-3553. https://doi.org/10.1007/s11277-021-09302-5

[12] Tumuluru, V. K., Wang, P., Niyato, D. Channel status prediction for cognitive radio networks. *Wireless Communications and Mobile Computing*. 2012, 12, 862-874. https://doi.org/10.1002/wcm.1017

[13] Bujunuru, A., Srinivasulu, T. A survey on spectrum sensing techniques and energy harvesting. *In IEEE International Conference on Recent Innovations in Electrical, Electronics, and Communication Engineering (ICRIEECE)*. Bhubaneswar, India, 2020. https://doi.org/10.1109/ICRIEECE44171.2018.9009159

[14] Gavrilovska, L., Atanasovski, V. Spectrum Sensing Framework for Cognitive Radio Networks. *Wireless Personal Communications*. 2011, 59, 447-469. https://doi.org/10.1007/s11277-011-0239-1

[15] Bhowmick, A., Prasad, B., Roy, S. D., Kundu, S. Performance of cognitive radio network with novel hybrid spectrum access schemes. *Wireless Personal Communications*. 2016, 91, 541-560. https://doi.org/10.1007/s11277-016-3476-5

[16] Awin, F., Raheem, E. A., Tepe, K. Blind spectrum sensing approaches for interweaved cognitive radio system: a tutorial and short course, *IEEE Communications Surveys and Tutorials*. 2019, 21(1), 238-259. https://doi.org/10.1109/COMST.2018.2863681

[17] Prathan, P. M., Panda, G. Information Combining Schemes for Cooperative Spectrum Sensing: A Survey and Comparative Performance Analysis. *Wireless Personal Communications*. 2017, 94, 685-711. https://doi.org/10.1007/s11277-016-3645-6

[18] Ali, A., Hamouda, W. Advances on spectrum sensing for cognitive radio networks: theory and applications. *IEEE Communications Surveys and Tutorials*. 2016, 19(2), 1277-1304. https://doi.org/10.1109/COMST.2016.2631080

[19] Claudino, L., AbrÃ£o, T. Spectrum Sensing Methods for Cognitive Radio Networks: A Review. *Wireless Personal Communications*. 2017, 95, 5003-5037. https://doi.org/10.1007/s11277-017-4143-1

[20] Chaudhari, S., Kosunen, M., Mäkinen, S., Oksanen, J., Laatta, M., Ojaniemi, J., Koivunen, V., Ryynänen, J. Valkama, M. Performance evaluation of Cyclostationary-Based Cooperative sensing Using field measurements. *IEEE Transactions on Vehicular Technology*. 2016, 65(4), 1982-1997. https://doi.org/10.1109/TVT.2015.2422715

[21] Kay, S. M. *Fundamentals of Statistical Signal Processing: Detection Theory*. Prentice Hall; 1993.

[22] Zhang, X., Gao, F., Chai, R., Jiang, T. Matched filter based spectrum sensing when primary user has multiple power levels. *Cnina Communications*. 2015, 12(2), 21-31. https://doi.org/10.1109/CC.2015.7084399

[23] Digham, F. F., Alouini, M. S., Simon, M. K. On the energy detection of unknown signals over fading channels. *IEEE Transactions on Communications*. 2007, 55(1), 21-24. https://doi.org/10.1109/TCOMM.2006.887483

[24] Chatziantoniou, E., Allen, B., Velisavljevic, V., Karadimas, P., Coon, J. Energy detection based spectrum sensing over two-wave with diffuse power fading channels. *IEEE Transactions on Vehicular Technology*. 2017, 66(1), 868-874. https://doi.org/10.1109/TVT.2016.2556084

[25] Sofotasios, P. C., Rebeiz, E., Zhang, L., Tsiftsis, T. A., Cabric, D., Freear, S. Energy detection based spectrum sensing over kappa-mu and kappa-mu extreme fading channels. *IEEE Transactions on Vehicular Technology*. 2013, 62(3), 1031-1040. https://doi.org/10.1109/TVT.2012.2228680

[26] De, P., Liang, Y. C. Blind spectrum sensing algorithms for cognitive radio networks. *IEEE Transactions on Vehicular Technology*. 2008, 57(5), 2834-2842. https://doi.org/10.1109/TVT.2008.915520

[27] Han, W., Huang, C., Li, J., Li, Z., Cui, S. Correlation-based spectrum sensing with oversampling in cognitive radio. *IEEE Journal of Selected Areas in Communications*. 2015, 33(5), 788-802. https://doi.org/10.1109/JSAC.2014.2361076

[28] Lunden, J., Kassam, S. A., Koivunen, V. Robust Nonparametric Cyclic Correlation-Based Spectrum Sensing for Cognitive Radio. *IEEE Transactions on Signal Processing*. 2010, 58(1), 38-52. https://doi.org/10.1109/TSP.2009.2029790

[29] Chaudhari, S., Koivunen, V., Poor, H. V. Distributed autocorrelation-based sequential detection of OFDM signals in cognitive radios. *In Proceedings of IEEE International Conference on Cognitive Radio Oriented Wireless Networks and Communications (CROWNCOM)*. Singapore, 2008; pp. 1-6. https://doi.org/10.1109/CROWNCOM.2008.4562525

[30] Chaudhari, S., Koivunen, V., Poor, H. V. Autocorrelation-based decentralized sequential detection of OFDM signals in cognitive radios. *IEEE Transactions on Signal Processing*. 2009, 57(7), 2690-2700. https://doi.org/10.1109/TSP.2009.2019176

[31] Chambers, P., Sellathurai, M. Implementation of an autocorrelation-based spectrum sensing algorithm in real-world channels with frequency offset. *In Proceedings of IEEE Sensor Signal Processing for Defense (SSPD)*. Edinburgh, UK, 2014; pp. 1-5. https://doi.org/10.1109/SSPD.2014.6943321

[32] Chin, W. L., Kao, C. W., Qian, Y. Spectrum sensing of OFDM systems over multipath fading channels and practical considerations for cognitive radios. *IEEE Sensors Journal*. 2016, 16(8), 2349-2360. https://doi.org/10.1109/JSEN.2016.2514405

[33] Haque, M, Shimamura, T. Performance evaluation of spectrum sensing for OFDM systems using parallel combination of comb filter and autocorrelator. *International Symposium on Intelligent Signal Processing and Communication Systems (ISPACS).* IEEE: Ishigaki, Japan, 2019; pp. 111-116. https://doi.org/10.1109/ISPACS.2018.8923151

[34] Socheleau, F. X., Bey, A. A. E., Houcke, S. Non data-aided SNR estimation of OFDM signals. *IEEE Communications Letters*. 2008, 12(11), 813-815. https://doi.org/10.1109/LCOMM.2008.081134

[35] Talbot, S. L., Boroujeny, B. F. Spectral method of blind carrier tracking for OFDM. *IEEE Transactions on Signal Processing*. 2008, 56(7), 2706-2717. https://doi.org/10.1109/TSP.2008.917377

[36] Hong, E., Kim, K., Har, D. Spectrum sensing by parallel pairs of cross-correlations and comb filters for OFDM systems with pilot tones. *IEEE Sensors Journal*. 2012, 12(7), 2380-2383. https://doi.org/10.1109/JSEN.2012.2188792

[37] Tandra, R., Sahai, A. SNR walls for signal detection. *IEEE Journal of Selected Topics in Signal Processing*. 2008, 2, 4-17. https://doi.org/10.1109/JSTSP.2007.914879